

A HEPATITIS B AND C VIRUS MODEL WITH AGE SINCE INFECTION THAT EXHIBITS BACKWARD BIFURCATION*

REDOUANE QESMI[†], SUSIE ELSAADANY[‡], JANE MARIE HEFFERNAN[§], AND
JIANHONG WU[§]

Abstract. We propose a mathematical model describing the dynamics of hepatitis B or C virus infection. The method of characteristics reduces the age-structured model to a system of differential equations with distributed delay. The model is rigorously analyzed, and a detailed stability analysis is performed. The model, consisting of two mutually exclusive compartments representing the interaction of the virus in the liver and the blood, has a locally asymptotically stable disease-free equilibrium (DFE) whenever a certain epidemiological threshold, known as the basic reproduction number R_0 , is less than unity. A sufficient condition for the global asymptotic stability of the trivial steady state is obtained. Further, under biologically realistic hypotheses, the model exhibits the phenomenon of backward bifurcation, where the stable DFE coexists with a stable endemic equilibrium. This means that reducing the basic reproduction number R_0 below 1 is not always sufficient to control HBV/HCV infection when the virus interacts with cells in both the liver and the blood. Numerical analysis confirms the results and stresses the role of some parameters involved in the elimination and persistence of the infection.

Key words. HBV, HCV, transplantation, functional differential equation, distributed delay, reinfection, equilibria, forward bifurcation, backward bifurcation

AMS subject classifications. 34D20, 34K20, 34K99, 92C37

DOI. 10.1137/10079690X

1. Introduction. Hepatitis B virus (HBV) and hepatitis C virus (HCV) are viruses that infect liver cells (hepatocytes) and can lead to acute infection, where virus is cleared from the body by the immune response, or chronic infection, where virus persists, leading to liver diseases such as cirrhosis and hepatocellular carcinoma [17]. It is reported that about 530 million people worldwide have long-term HBV or HCV infection [29, 4] and at least an estimated 600,000 persons die each year due to the acute or chronic consequences of these infections [38].

Current HBV and HCV drug therapies (such as Peginterferon- α Cribavirin for HCV and lamivudine (LMV) and entecavir for HBV) produce a range of cure rates, from 13–46% for HCV patients, and a similar amount for HBV [18, 10, 22]. However, liver transplantation in end-stage HCV/HBV-related liver disease is currently the only life-saving alternative but is unsuccessful since HBV/HCV reinfection of the liver graft often results in a rapidly progressive course of disease. Historically, in the absence of prevention, the spontaneous risk for HBV reinfection after transplantation of approximately 80% is related to the initial liver disease and the presence of HBV replication at time of transplantation [11, 35]. This almost inevitable post-

*Received by the editors June 1, 2010; accepted for publication (in revised form) March 16, 2011; published electronically August 25, 2011.

<http://www.siam.org/journals/siap/71-4/79690.html>

[†]Department of Mathematics and Statistics, York University, 4700 Keele Street, Toronto, ON, M3J 1P3, Canada (rqesm@mathstat.yorku.ca).

[‡]Blood Safety Surveillance and Health Care Acquired Infections, Division Centre for Communicable Diseases and Infection Control, Public Health Agency of Canada, Ottawa, ON, K1A 0L2, Canada (susie.elsaadany@phac-aspc.gc.ca).

[§]MITACS Centre for Disease Modelling and Department of Mathematics and Statistics, York University, 4700 Keele Street, Toronto, ON, M3J 1P3, Canada (jmheffer@mathstat.yorku.ca, wujh@mathstat.yorku.ca).

transplant infection may be related to the existence of an extra-hepatic replication compartment such as the blood [21]. Indeed, based on the work in [3], it is obvious that HCV particles experience a relatively large flux and undergo replication in cells, such as PBMCs, that circulate in the blood. This kind of information is less available for HBV. However, it is shown in [1] that although the pathophysiology of extra-hepatic manifestations in HBV is not completely understood, between the circulation of immune-complex deposits in the blood and the proof of viral replication in the vascular endothelium, the blood is a compartment of infection/viral replication similar enough to HCV.

Viral infection models for HBV and HCV have been considered by several authors (see [25] and [28, 26]). Recently, Qesmi et al. [30] extended the basic model of viral dynamics (see Nowak and May [26] and Perelson et al. [28]) by incorporating two features, namely, the blood cells (e.g., PBMC such as B cells and T cells) as the second compartment of HBV/HCV infection and the loss of virions during the infection process. The second feature plays a major role in HBV/HCV dynamics, especially when the viral load is small, i.e., when a patient is under drug therapy [15]. Qesmi et al. [30] proved that by including the second compartment of infection (the blood), persistence of HBV/HCV in chronically infected patients could be found even if drug therapies are effective in reducing viral replication in the liver. However, the single compartmental model approach could not demonstrate such a phenomenon. Furthermore, Qesmi et al. [30] demonstrated that the two compartment model shows the existence of a bistability phenomenon. This determines a quantitative estimation of the responsible factors/parameters of viral persistence under drug therapy regimens and can lead to important conclusions regarding therapies needed after liver transplantation.

Most in-host models of infectious diseases have assumed that infected cells produce virus particles at a constant rate during their lifetime and that their death rate is constant [28, 27, 26]. These are not realistic assumptions in terms of HBV and HCV infection. First, HBV and HCV are nonlytic viruses. Thus, the death rate of infected cells during HBV or HCV infection depends on the activation of the immune system and when infected cells demonstrate on their cell surface that they are indeed infected. Thus, it is reasonable to assume that the probability of infected cell death, which occurs by the killing of infected cells by immune system components such as CD8 T-cells, is small early in the life of an infected cell and that this ramps up to a maximum death rate over time. Also, since virus particles in HBV and HCV exit the host cell via exocytosis with progeny gradually budding out of the plasma membrane in the beginning of infection up to a maximal bud rate until cell death [9], it is not realistic to assume that virus production by an infected cell occurs at a constant rate over the lifetime of the cell. Instead, the production of new virus particles ramps up as viral proteins and genetic information accumulate within the cytoplasm [2, 26]. Nelson et al. [24] introduced an age-structured generalization of the basic model of viral dynamics [26, 28], where the infected cell population is structured by the age since infection, i.e., the time that has passed since the moment of infection of the cell by a virion.

In this study we extend the model of Qesmi et al. [30] to include age structure similar to that of Nelson et al. [24]. This formulation makes it possible to study the HBV/HCV model in general cases, instead of considering a constant production rate of viral particles and constant death rate of infected cells as assumed in the previous ODE model [30]. It also allows us to introduce and evaluate the efficacy of control mechanisms of HBV/HCV infection. Furthermore, the model is a useful tool, which

in future work will be used to predict the level of infection of target cells in the blood that are needed to reinfect a new liver after transplantation, under timescales observed in transplant patients.

We consider a general form of the production rate of the viral particles and the death rate of infected cells. In addition, we establish the global stability of the disease-free equilibrium (DFE) and show the appearance of both forward and backward bifurcations. The last scenario, known as the bistable phenomenon, has been explored in many epidemic models (see [12] and references therein for models in vivo and [7, 8, 13] for epidemiological models). However, to the best of our knowledge, few modeling studies have highlighted backward bifurcation for age-structured models (see [20, 31], for instance). This type of bifurcation behavior allows for the existence of multiple positive steady states, leading to different threshold conditions for the onset of an infection and its elimination. In particular, control measures reducing the basic reproduction number are not as effective as in the case of the absence of backward bifurcation. This has clear implications toward drug therapy strategies before, after, and during liver transplantation. We also find that the incorporation of age since infection does not change the qualitative behaviour dramatically.

The paper is organized as follows: Section 2 is devoted to the presentation of the model, which originally takes the form of an age-structured system. This system is then reduced to a system of delay differential equations. In section 3, we calculate the basic reproduction number using the survival method. In section 4, we focus on the equilibria and prove a sufficient condition for the global asymptotic stability of the DFE. Next, we linearize the system about the DFE and show its instability when R_0 exceeds 1. We perform the analysis of the forward bifurcation as well as backward bifurcation in section 5. Detailed numerical simulations that support or complete our analytical results are presented in section 6. In section 7 we discuss the results and their effects on the biological system in question and propose some future work.

2. The model of HBV/HCV dynamics. The population is divided into five classes: healthy cells in the liver and blood ($x(t)$ and $z(t)$, respectively), infected cells in the liver and blood structured by the age a of infection ($y(a, t)$ and $w(a, t)$, respectively), and virus concentration (v). The model is given by the following system of differential equations:

$$(2.1) \quad \begin{cases} \frac{dx}{dt} = \lambda_x - \beta_x xv - d_x x, \\ \frac{\partial y}{dt} + \frac{\partial y}{da} = -\eta_y(a)y(a, t), \\ \frac{dv}{dt} = \int_0^\infty k_y(a)y(a, t)da + \int_0^\infty k_w(a)w(a, t)da - \beta_x xv - \beta_z zv - uv(t), \\ \frac{dz}{dt} = \lambda_z - \beta_z zv - d_z z, \\ \frac{\partial w}{dt} + \frac{\partial w}{da} = -\eta_w(a)w(a, t), \end{cases}$$

subject to the boundary condition describing the production of the infected cells:

$$(2.2) \quad y(0, t) = \beta_x x(t)v(t), \quad w(0, t) = \beta_z z(t)v(t).$$

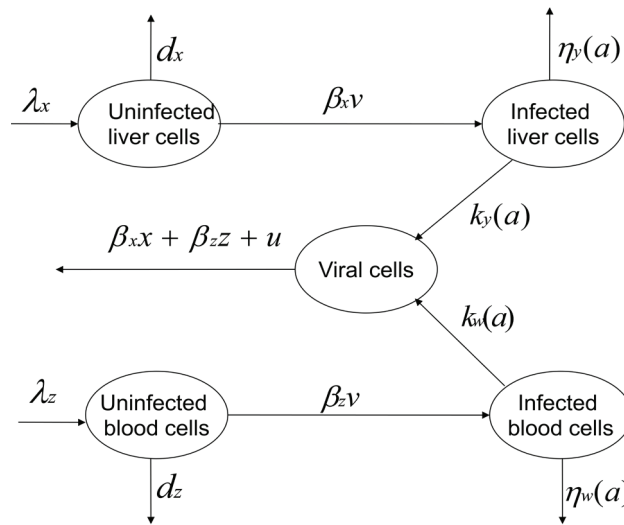


FIG. 1. Flow diagram of HBV/HCV liver-virus-blood model structure.

In this model, target cells in the liver (blood) are produced at a constant rate λ_x (λ_z) and die at a constant rate d_x (d_z). *De novo* infection occurs in the liver (blood) at a constant rate β_x (β_z), and infected cells in the liver (blood) of age a die at a rate $\eta_y(a)$ ($\eta_w(a)$). HBV/HCV is produced by infected liver (blood) cells of age a at an average rate $k_y(a)$ ($k_w(a)$). The virus is cleared with a rate constant u , and it is lost when it infects a healthy cell [15]. The dynamics of the system are schematically illustrated in Figure 1.

Note that system (2.1) only splits the healthy and infected cell populations into two compartments depending on their location (the blood or the liver). We have elected, however, to assume only one virus compartment which accounts for virus in both the liver and the blood. We believe that this is a reasonable assumption since (a) the transfer rates between the liver and the blood of virus particles is unknown, and (b) since the blood circulates around the body very quickly we can assume that the virus compartment is well mixed. For example, using current measurements of liver perfusion in healthy and chronically infected individuals with HBV or HCV, we can determine that approximately 400 to over 4000 L of blood goes through the liver every day (the lower bound corresponds to people with liver fibrosis, and the upper bound corresponds to healthy individuals) [37, 33]. This means that every 1 to 20 minutes, 5L of blood goes through the liver. Since the volume of blood in the human body is approximately 5L, we can then assume that the probability that a virus particle in the blood will reach the liver is VERY high, and thus one compartment for the virus is a reasonable assumption.

The limitation of viral protein produced in the infected cells requires that the rates of the virus, $k_y(a)$ and $k_w(a)$, are integrable in $[0, \infty)$. Standard arguments can be used to prove the existence and uniqueness of solutions to the system (2.1) subject to initial conditions: $x(0), v(0), z(0) \in [0, \infty)$ and $y(\cdot, 0), w(\cdot, 0) \in L([0, \infty), [0, \infty))$ (see, for example, [19, 36]). In addition, we can show that $x(t)$, $z(t)$, $v(t)$, $y(a, t)$, and $w(a, t)$ are nonnegative and bounded for $t \geq 0$ and $a \geq 0$.

Define, for $a \geq 0$, the functions

$$(2.3) \quad \sigma_y(a) = e^{-\int_0^a \eta_y(s) ds} \quad \text{and} \quad \sigma_w(a) = e^{-\int_0^a \eta_w(s) ds},$$

and let N_y and N_w be the constants given by

$$(2.4) \quad N_y = \int_0^\infty k_y(a)\sigma_y(a)da \quad \text{and} \quad N_w = \int_0^\infty k_w(a)\sigma_w(a)da.$$

The constants N_y and N_w give the total numbers of viral particles produced over the lifespan of an infected cell in the liver and the blood, and these are called the burst sizes. $\sigma_y(a)$ and $\sigma_w(a)$ are the probability an infected cell survives to age a . Using the integration along characteristics (see [36]), one can show that system (2.1) can be reduced to the following system of delay differential equations:

$$(2.5) \quad \begin{cases} \frac{dx}{dt} = \lambda_x - \beta_x xv - d_x x, \\ \frac{dv}{dt} = \beta_x \int_0^t k_y(a)\sigma_y(a)v(t-a)x(t-a)da - \beta_x xv \\ \quad + \beta_z \int_0^t k_w(a)\sigma_w(a)v(t-a)z(t-a)da - \beta_z zv - uv(t) + F(t), \\ \frac{dz}{dt} = \lambda_z - \beta_x xv - d_z z, \end{cases}$$

where

$$F(t) = \int_t^\infty (k_y(a)\sigma_y(a)\sigma_y(t-a)y(a-t,0) + k_w(a)\sigma_w(a)\sigma_w(t-a)w(a-t,0)) da,$$

and $F(t)$ converges to zero as t tends to infinity. Therefore, the qualitative behavior of the solutions of system (2.5) is given by its limiting system (see [23])

$$(2.6) \quad \begin{cases} \frac{dx}{dt} = \lambda_x - \beta_x xv - d_x x, \\ \frac{dv}{dt} = \beta_x \int_0^\infty k_y(a)\sigma_y(a)v(t-a)x(t-a)da - \beta_x xv \\ \quad + \beta_z \int_0^\infty k_w(a)\sigma_w(a)v(t-a)z(t-a)da - \beta_z zv - uv(t), \\ \frac{dz}{dt} = \lambda_z - \beta_x xv - d_z z. \end{cases}$$

This is a nonlinear system of differential equations with distributed delay. Indeed, the functions $k_y(\cdot)\sigma_y(\cdot)$ and $k_w(\cdot)\sigma_w(\cdot)$ are nonnegative and integrable on $[0, \infty)$. Furthermore, without loss of generality one could assume that $k_y(\cdot)\sigma_y(\cdot)$ and $k_w(\cdot)\sigma_w(\cdot)$ are density functions. Although model (2.1) is the main model describing the viral dynamics with age, the distributed delay model (2.6) is meaningful in the sense that it preserves the same dynamic and the characteristics of the main model. Thus, hereafter, we will concentrate on the study of model (2.6).

3. Basic reproduction number. The basic reproduction number is defined as the average number of secondary infections produced when one infected individual is introduced into a host virgin population [6, 7, 14]. To compute this number, we apply the *survival function* approach described by Heffernan, Smith, and Wahl [14].

Let \bar{x} and \bar{z} denote the healthy cell populations in the liver and blood in the absence of infection, i.e., the population of cells when the liver and blood are not infected yet. It is easy to check that \bar{x} and \bar{z} are given explicitly and successively by $\frac{\lambda_x}{d_x}$ and $\frac{\lambda_z}{d_z}$; see also section 4. Let $F_x(s)$ ($F_z(s)$) be the probability that a newly infected liver (blood) cell has been produced by an infectious virion in the liver (blood) and lives for at least time s . Then the probability function $F_x(s)$ can be expressed as

$$F_x(s) = \int_0^s P_1(t) \cdot P_2(t) \cdot P_3(s, t) dt,$$

where $P_1(t)$ is the probability that a virion in the liver produced at time 0 exists at time t and, assuming an exponential distribution, is given by $e^{-(u+\beta_x\bar{x}+\beta_z\bar{z})t}$; $P_2(t)$ is the rate at which a virion which has existed for time t infects and is given by $\beta_x\bar{x}$; and $P_3(s, t)$ is the probability that an infected cell in the liver lives to age $s - t$ and is given by $e^{-\int_t^s \eta_y(a) da}$. Similarly, we define the probability function $F_z(s)$.

Now, let $b_y(s)$ and $b_w(s)$ be the average number of virions produced by a liver or blood cell which has been infected for time s [16]. Then $b_y(s) = k_y(s)$ and $b_w(s) = k_w(s)$.

R_0 is defined by the following integral:

$$(3.1) \quad R_0 = \int_0^\infty [b_y(s)F_x(s) + b_w(s)F_z(s)] ds.$$

Substituting the values of $b_y(s)$, $b_w(s)$, $F_y(s)$, and $F_w(s)$ into (3.1), we obtain

$$(3.2) \quad R_0 = \int_0^\infty k_y(s) \int_0^s \beta_x \bar{x} e^{-(u+\beta_x\bar{x}+\beta_z\bar{z})t} e^{-\int_t^s \eta_y(a) da} dt ds \\ + \int_0^\infty k_w(s) \int_0^s \beta_z \bar{z} e^{-(u+\beta_x\bar{x}+\beta_z\bar{z})t} e^{-\int_t^s \eta_w(a) da} dt ds,$$

which, after interchanging the integrals, is reduced to

$$(3.3) \quad R_0 = N_y \beta_x \frac{\bar{x}}{u + \beta_x \bar{x} + \beta_z \bar{z}} + N_w \beta_z \frac{\bar{z}}{u + \beta_x \bar{x} + \beta_z \bar{z}}.$$

The value of the basic reproduction number, R_0 , defined above plays a central role in the dynamics of system (2.6) with important implications for the treatment of HBV/HCV. The parameter R_0 has an interesting biological interpretation in this context: assume that an initial virus load V_0 is introduced in a healthy organism with \bar{x} healthy liver cells and \bar{z} healthy blood cells. These viruses produce an average of $\frac{\beta_x \bar{x}}{u + \beta_x \bar{x} + \beta_z \bar{z}} V_0$ infected liver cells and $\frac{\beta_z \bar{z}}{u + \beta_x \bar{x} + \beta_z \bar{z}} V_0$ infected blood cells during their lifespan. Since each infected liver cell and infected blood cell produces N_y virion and N_w virion during its lifespan, $(N_y \frac{\beta_x \bar{x}}{u + \beta_x \bar{x} + \beta_z \bar{z}} + N_w \frac{\beta_z \bar{z}}{u + \beta_x \bar{x} + \beta_z \bar{z}}) V_0 = R_0 V_0$ is the average number of new virions produced by the initial virion in a healthy organism.

Remark 1. It is easy to show that the value of R_0 , given by (3.3), can be reduced to the basic reproduction number obtained in [30] by assuming that both the production rate k and the death rate η are constants.

4. Steady states and disease extinction. Let $E = (x_e, v_e, z_e)$ represent an arbitrary equilibrium of the model (2.6). Then

$$(4.1) \quad x_e = \frac{\lambda_x}{\beta_x v_e + d_x}, \quad z_e = \frac{\lambda_z}{\beta_z v_e + d_z},$$

and

$$(4.2) \quad h(v_e) = (Av_e^2 + Bv_e + C)v_e = 0,$$

where

$$(4.3) \quad A = u\beta_x\beta_z,$$

$$(4.4) \quad B = ud_z\beta_x + ud_x\beta_z + \lambda_x\beta_x\beta_z(1 - N_y) + \lambda_z\beta_x\beta_z(1 - N_w),$$

$$(4.5) \quad C = ud_xd_z + \lambda_x\beta_xd_z(1 - N_y) + \lambda_z\beta_zd_x(1 - N_w).$$

In particular, system (2.6) always has the DFE

$$E_f = (\bar{x}, 0, \bar{z}) = \left(\frac{\lambda_x}{d_x}, 0, \frac{\lambda_z}{d_z} \right),$$

whereas the existence of an endemic equilibrium depends on the values of the parameters A , B , and C . Since $A > 0$, the existence of a positive solution, v_e , of (4.2) depends on the signs of B and C . Note that

$$(4.6) \quad C = (u + \beta_x\bar{x} + \beta_z\bar{z})(1 - R_0).$$

Therefore, $C < 0$ if and only if $R_0 > 1$. Thus, we state the following theorem.

THEOREM 4.1. *System (2.6) has*

- (i) *a unique endemic equilibrium if $C < 0$;*
- (ii) *a unique endemic equilibrium if $B < 0$, and $C = 0$ or $B^2 - 4AC = 0$;*
- (iii) *two endemic equilibria if $C > 0$, $B < 0$, and $B^2 - 4AC > 0$;*
- (iv) *no endemic equilibrium if conditions (i)–(iii) are not satisfied.*

The following remark discusses the above theorem in terms of parameters of system (2.6). This is useful in the next sections of the paper.

Remark 2. It is easy to show that

$$(4.7) \quad d_xd_zB = (\beta_xd_z + \beta_zd_x)C + \beta_x^2d_z^2\lambda_x(N_y - 1) + \beta_z^2d_x^2\lambda_z(N_w - 1).$$

Thus, $B \geq 0$ whenever $C \geq 0$, $N_y \geq 1$, and $N_w \geq 1$. On the other hand, from (4.4) and (4.5), $B \geq 0$ and $C \geq 0$ for $N_y \leq 1$ and $N_w \leq 1$. Hence, system (2.6) has no endemic equilibrium if $R_0 \leq 1$ and $(N_y - 1)(N_w - 1) \geq 0$. This illuminates the case (iv). However, if $(N_y - 1)(N_w - 1) < 0$, then it is obvious that both B and C change signs for some parameters of system (2.6). Consequently, cases (ii) and (iii) of Theorem 4.1 are possible in this case, i.e., $(N_y - 1)(N_w - 1) < 0$. Finally, we can remark that case (i) holds true for all parameters of system (2.6) for which $R_0 > 1$.

The stability properties of the endemic equilibria will be discussed in the next section. Here we consider only the case when $R_0 < 1$. In this case, only the DFE E_f exists, and the disease goes to extinction. More precisely, we have the following theorem.

THEOREM 4.2. *Assume that $R_0 < 1$ and $(N_y - 1)(N_w - 1) \geq 0$. Then, the disease-free steady state E_f of system (2.6) is a global attractor; i.e.,*

$$\lim_{t \rightarrow \infty} (x(t), v(t), z(t)) = (\bar{x}, 0, \bar{z})$$

for any positive solution $(x(t), v(t), z(t))$ of system (2.6).

To prove Theorem 4.2, we need the following lemmas, where, for any bounded real-valued function f on $[0, \infty)$, we rewrite

$$f_\infty = \liminf_{t \rightarrow \infty} f(t) \text{ and } f^\infty = \limsup_{t \rightarrow \infty} f(t).$$

LEMMA 4.3. *Let $f : [0, \infty) \rightarrow \mathbb{R}$ be bounded, and let $K \in L^1(0, \infty)$; then*

$$\limsup_{t \rightarrow \infty} \left| \int_0^\infty K(\theta) f(t - \theta) d\theta \right| \leq |f^\infty| \|K\|_{L^1(0, \infty)}.$$

LEMMA 4.4 (see [34]). *Let $f : [0, \infty) \rightarrow \mathbb{R}$ be bounded and twice differentiable with bounded second derivative. Let $t_n \rightarrow \infty$ be given so that $f(t_n)$ converge to f^∞ or f_∞ as $n \rightarrow \infty$. Then the derivative f' of the function f satisfies*

$$f'(t_n) \rightarrow 0 \text{ as } n \rightarrow \infty.$$

Proof of Theorem 4.2. Let $(x(t), v(t), z(t))$ be a positive solution of system (2.6) and consider the function

$$(4.8) \quad G(t) = \begin{cases} \beta_x \int_0^\infty k_y(a) \sigma_y(a) v(t-a) x(t-a) da \\ + \beta_z \int_0^\infty k_w(a) \sigma_w(a) v(t-a) z(t-a) da. \end{cases}$$

Using Lemma 4.3, we have

$$(4.9) \quad \begin{aligned} & \beta_x \limsup_{t \rightarrow \infty} \int_0^\infty k_y(a) \sigma_y(a) v(t-a) x(t-a) da \\ & \leq \beta_x x^\infty v^\infty \int_0^\infty k_y(a) \sigma_y(a) da \\ & = \beta_x x^\infty v^\infty N_y. \end{aligned}$$

Similarly, we have

$$\beta_z \limsup_{t \rightarrow \infty} \int_0^\infty k_w(a) \sigma_w(a) v(t-a) z(t-a) da \leq \beta_z z^\infty v^\infty N_w.$$

Then

$$\limsup_{t \rightarrow \infty} G(t) \leq (\beta_x x^\infty N_y + \beta_z z^\infty N_w) v^\infty.$$

Using Lemma 4.4, we can choose a sequence $t_n \rightarrow \infty$ such that $v(t_n) \rightarrow v^\infty$ and $\dot{v}(t_n) \rightarrow 0$. Then from the v -equation in (2.6), we can take \limsup to get

$$(\beta_x x^\infty + \beta_z z^\infty + u) v^\infty = \limsup_{t \rightarrow \infty} G(t) \leq (\beta_x x^\infty N_y + \beta_z z^\infty N_w) v^\infty,$$

or equivalently

$$(4.10) \quad (\beta_x x^\infty (N_y - 1) + \beta_z z^\infty (N_w - 1) - u) v^\infty \geq 0.$$

If $N_y \leq 1$ and $N_w \leq 1$, the above inequality holds only if $v^\infty = 0$.

Now, assume that $N_y \geq 1$ and $N_w \geq 1$. Integrating the first and the third equations in (2.6) and then taking the lim sup, we obtain

$$x^\infty \leq \frac{\lambda_x}{d_x} = \bar{x} \quad \text{and} \quad z^\infty \leq \frac{\lambda_z}{d_z} = \bar{z}.$$

Then, from (4.10), it follows that $(\beta_x \bar{x}(N_y - 1) + \beta_z \bar{z}(N_w - 1) - u)v^\infty \geq 0$. Thus,

$$(\beta_x \bar{x} + \beta_z \bar{z} + u)(R_0 - 1)v^\infty \geq 0.$$

Since $R_0 < 1$, the last inequality is true only if $\limsup_{t \rightarrow \infty} v(t) = 0$. Consequently, $\lim_{t \rightarrow \infty} v(t) = 0$. Furthermore, integrating the first and the third equations in (2.6) and taking the limit, we obtain

$$\lim_{t \rightarrow \infty} x(t) = \frac{\lambda_x}{d_x} = \bar{x} \quad \text{and} \quad \lim_{t \rightarrow \infty} z(t) = \frac{\lambda_z}{d_z} = \bar{z}.$$

The proof of Theorem 4.2 is complete.

5. Stability and bifurcation analysis. In this section, we consider the case in which conditions in Theorem 4.2 are not fulfilled and new equilibria other than E_f exist.

5.1. Instability of DFE. We first note the following.

THEOREM 5.1. *The DFE E_f is unstable if $R_0 > 1$.*

Proof. Linearizing system (2.6) at the DFE $E_f = (\bar{x}, 0, \bar{z})$ gives the following linear system:

$$\left\{ \begin{aligned} \frac{dX(t)}{dt} &= -d_x X(t) - \beta_x \bar{x} V(t), \\ \frac{dV(t)}{dt} &= \int_0^\infty (k_y(a)\sigma_y(a)\beta_x \bar{x} + k_w(a)\sigma_w(a)\beta_z \bar{z}) V(t-a) da \\ &\quad + \beta_x \int_0^\infty k_y(a)\sigma_y(a) X(t-a) da \\ &\quad + \beta_z \int_0^\infty k_w(a)\sigma_w(a) Z(t-a) da - \beta_x \bar{v} X(t) - \beta_z \bar{v} Z(t) \\ &\quad - (\beta_x \bar{x} + \beta_z \bar{z}) V(t) - uV(t), \\ \frac{dZ(t)}{dt} &= -d_z Z(t) - \beta_z \bar{z} V(t). \end{aligned} \right.$$

Substituting the ansatz $E_0 e^{\lambda t}$, where $E_0 = (X_0, V_0, Z_0)$, leads to

$$\left\{ \begin{aligned} \lambda e^{\lambda t} X_0 &= -d_x e^{\lambda t} X_0 - \beta_x \bar{x} e^{\lambda t} V_0, \\ \lambda e^{\lambda t} V_0 &= \beta_x \int_0^\infty (k_y(a)\sigma_y(a)\beta_x \bar{x} + k_w(a)\sigma_w(a)\beta_z \bar{z}) e^{\lambda(t-a)} da V_0 \\ &\quad + \beta_x \int_0^\infty k_y(a)\sigma_y(a) e^{\lambda(t-a)} da X_0 + \beta_z \int_0^\infty k_w(a)\sigma_w(a) e^{\lambda(t-a)} da Z_0 \\ &\quad - \beta_x \bar{v} e^{\lambda t} X_0 - \beta_z \bar{v} Z_0 e^{\lambda t} - (\beta_x \bar{x} + \beta_z \bar{z}) e^{\lambda t} V_0 - u e^{\lambda t} V_0, \\ \lambda e^{\lambda t} Z_0 &= -d_z e^{\lambda t} Z_0 - \beta_z \bar{z} e^{\lambda t} V_0. \end{aligned} \right.$$

Without loss of generality, we may assume $V_0 = 1$. Eliminating $e^{\lambda t}$, we obtain $X_0 = -\frac{\beta_x \bar{x}}{\lambda + d_x}$ and $Z_0 = -\frac{\beta_z \bar{z}}{\lambda + d_z}$, where λ is a root of the characteristic function

$$\Delta_f(\lambda) = \lambda + \beta_x \bar{x} + \beta_z \bar{z} + u - \int_0^\infty (k_y(a)\sigma_y(a)\beta_x \bar{x} + k_w(a)\sigma_w(a)\beta_z \bar{z}) e^{-\lambda a} da.$$

Obviously, $\Delta_f(\lambda)$ is a monotonically increasing continuous function for nonnegative real λ and $\Delta_f(\infty) = \infty$. Furthermore, we have

$$\begin{aligned} \Delta_f(0) &= \beta_x \bar{x} + \beta_z \bar{z} + u - \int_0^\infty (k_y(a)\sigma_y(a)\beta_x \bar{x} + k_w(a)\sigma_w(a)\beta_z \bar{z}) da \\ &= (\beta_x \bar{x} + \beta_z \bar{z} + u) (1 - R_0). \end{aligned}$$

When $R_0 > 1$, we have $\Delta_f(0) < 0$, so there exists a positive real λ_0 such that $\Delta_f(\lambda_0) = 0$. This proves the instability of DFE. \square

In the following, we show that system (2.6) undergoes two possible options of bifurcation depending on the parameters chosen.

5.2. Forward transcritical bifurcation. In the following we consider the existence of a forward transcritical bifurcation when $N_y \geq 1$ and $N_w \geq 1$. For $R_0 > 1$, the equilibrium E_f becomes an unstable hyperbolic point, and the endemically infected equilibrium, denoted $E^* = (x^*, v^*, z^*)$, emerges.

For simplicity, we use the notation

$$N_y^\lambda = \int_0^\infty k_y(a)\sigma_y(a)e^{-\lambda a} da, \quad N_w^\lambda = \int_0^\infty k_w(a)\sigma_w(a)e^{-\lambda a} da.$$

The characteristic equation associated with the endemic equilibrium E^* is $\Delta_{E^*}(\lambda) = 0$, where

$$\begin{aligned} \Delta_{E^*}(\lambda) &= (\lambda + d_x + \beta_x v^*) (\lambda + d_z + \beta_z v^*) (\lambda + \beta_x x^* + \beta_z z^* + u - \beta_x x^* N_y^\lambda - \beta_z z^* N_w^\lambda) \\ (5.1) \quad &+ \beta_z^2 v^* z^* (\lambda + d_x + \beta_x v^*) (N_w^\lambda - 1) + \beta_x^2 v^* x^* (\lambda + d_z + \beta_z v^*) (N_y^\lambda - 1). \end{aligned}$$

THEOREM 5.2. *If $R_0 = 1$ and $N_y, N_w \geq 1$, then the endemically infected state E^* undergoes a forward transcritical bifurcation. That is, for $R_0 > 1$ and R_0 close to 1, the positive steady state, E^* , is locally asymptotically stable, whereas the DFE is unstable; and for $R_0 \leq 1$ the DFE is locally asymptotically stable and is the only steady state of (2.6).*

Proof. First, we prove that 0 is not a root of (5.1). We have $N_y^0 = N_y \geq 1$ and $N_w^0 = N_w \geq 1$. Since the endemic equilibrium $E^* = (x^*, v^*, z^*)$ satisfies the relation

$$(5.2) \quad \beta_x x^* + \beta_z z^* + u = \beta_x x^* N_y + \beta_z z^* N_w,$$

we have

$$\Delta_{E^*}(0) = \beta_x^2 v^* x^* (d_z + \beta_z v^*) (N_y - 1) + \beta_z^2 v^* z^* (d_x + \beta_x v^*) (N_w - 1) > 0.$$

Therefore, $\Delta_{E^*}(\lambda) = 0$ is equivalent to

$$(5.3) \quad (\lambda + d_x + \beta_x v^*) (\lambda + d_z + \beta_z v^*) (\lambda + \beta_x x^* + \beta_z z^* + u) = Q_1 + Q_2,$$

where

$$Q_1 = (\lambda + d_x)(\lambda + d_z + \beta_z v^*) N_y^\lambda \beta_x x^* + (\lambda + d_z + \beta_z v^*) \beta_x^2 x^* v^*$$

and

$$Q_2 = (\lambda + d_z)(\lambda + d_x + \beta_x v^*) N_w^\lambda \beta_z z^* + (\lambda + d_x + \beta_x v^*) \beta_z^2 z^* v^*.$$

Now, let $\lambda = \alpha + i\gamma$ be a root of $\Delta_{E^*}(\lambda)$ with $\alpha \geq 0$. Then $\lambda \neq 0$ and $|e^{-\lambda a}| \leq 1$ for any $a > 0$. Thus, $|N_y^\lambda| \leq N_y$ and $|N_w^\lambda| \leq N_w$. Therefore, since $N_y \geq 1$ and $N_w \geq 1$, we have

$$\begin{aligned} |Q_1|^2 &= |(\lambda + d_x)(\lambda + d_z + \beta_z v^*) N_y^\lambda \beta_x x^* + (\lambda + d_z + \beta_z v^*) \beta_x^2 x^* v^*|^2 \\ &= (\beta_x x^*)^2 |\lambda + d_z + \beta_z v^*|^2 |(\alpha + i\gamma + d_x) N_y^\lambda + \beta_x v^*|^2 \\ &\leq (\beta_x x^*)^2 |\lambda + d_z + \beta_z v^*|^2 (|(\alpha + d_x) N_y^\lambda + \beta_x v^*|^2 + |\gamma N_y^\lambda|^2) \\ &\leq (\beta_x x^*)^2 |\lambda + d_z + \beta_z v^*|^2 (|(\alpha + d_x) N_y + \beta_x v^* N_y|^2 + |\gamma N_y|^2) \\ &= (\beta_x x^*)^2 |\lambda + d_z + \beta_z v^*|^2 (|(\alpha + d_x) + \beta_x v^*|^2 + |\gamma|^2) N_y^2 \\ &= |(\lambda + d_z + \beta_z v^*)(\lambda + d_x + \beta_x v^*)|^2 (\beta_x x^* N_y)^2. \end{aligned}$$

Then

$$\begin{aligned} |Q_1| &= |(\lambda + d_x)(\lambda + d_z + \beta_z v^*) N_y^\lambda \beta_x x^* + (\lambda + d_z + \beta_z v^*) \beta_x^2 x^* v^*| \\ &\leq |(\lambda + d_z + \beta_z v^*)(\lambda + d_x + \beta_x v^*)| \beta_x x^* N_y. \end{aligned}$$

Similarly,

$$\begin{aligned} |Q_2| &= |(\lambda + d_z)(\lambda + d_x + \beta_x v^*) N_w^\lambda \beta_z z^* + (\lambda + d_x + \beta_x v^*) \beta_z^2 z^* v^*| \\ &\leq |(\lambda + d_x + \beta_x v^*)(\lambda + d_z + \beta_z v^*)| \beta_z z^* N_w. \end{aligned}$$

Using (5.3), we obtain

$$|\lambda + \beta_x x^* + \beta_z z^* + u| \leq \beta_x x^* N_y + \beta_z z^* N_w,$$

which is a contradiction to (5.2). Therefore, every root has negative real part, and, using Theorem 2.1 in [5], the endemic equilibrium E^* is locally asymptotically stable.

From Theorem 4.2, the DFE is globally asymptotically stable when $R_0 < 1$ and, from Theorem 5.1, is unstable when $R_0 > 1$. Thus the system (2.6) undergoes a forward bifurcation. \square

5.3. Backward bifurcation. The case (iii) indicates the possibility of a backward bifurcation (where the locally asymptotically stable DFE coexists with a locally asymptotically endemic equilibrium when $R_0 < 1$). To check for this, we set the discriminant $B^2 - 4AC$ to zero and solve for the critical value of R_0 (denoted R_c) as follows:

$$R_c = 1 - \frac{B^2}{4A(u + \beta_x \bar{x} + \beta_z \bar{z})}.$$

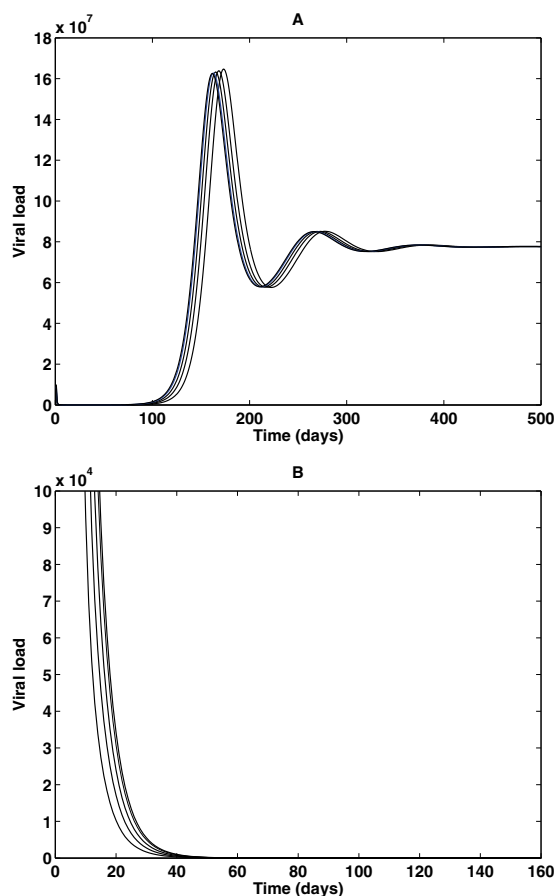


FIG. 2. Time series plot using different initial conditions for the initial viral load (V_0) of the model (2.1) with $R_0 = 0.97$. Figure A corresponds to the stable endemic equilibrium with $V_0 \in \{3 \times 10^6, 5 \times 10^6, 7 \times 10^6, 9 \times 10^6, 10 \times 10^6\}$, whereas Figure B accounts for the stable DFE with $V_0 \in \{10^6, 1.5 \times 10^6, 2 \times 10^6, 2.5 \times 10^6, 2.7 \times 10^6\}$.

Thus, $R_c < R_0$ is equivalent to $B^2 - 4AC > 0$, and, therefore, there exist two endemic equilibria, $E_m = (x_m, v_m, z_m)$ and $E_M = (x_M, v_M, z_M)$, such that

$$(5.4) \quad x_M = \frac{\lambda_x}{d_x + \beta_x v_M}, \quad v_M = \frac{-B + \sqrt{B^2 - 4AC}}{2A}, \quad z_M = \frac{\lambda_z}{d_z + \beta_z v_M}$$

and

$$x_m = \frac{\lambda_x}{d_x + \beta_x v_m}, \quad v_m = \frac{-B - \sqrt{B^2 - 4AC}}{2A}, \quad z_m = \frac{\lambda_z}{d_z + \beta_z v_m}.$$

Hence, a backward bifurcation occurs for values of R_0 such that $R_c < R_0 < 1$. This will be illustrated by simulating the model with a set of parameter values. A time series of the virus, v , is plotted in Figure 2, showing the coexistence of the DFE (corresponding to $v = 0$) and an endemic equilibrium (corresponding to $v = 7.9 \times 10^7$) for $R_0 = 0.97$. Further, Figure 2 shows that the endemic equilibrium and the DFE are both locally asymptotically stable.

In the following, we will prove the existence of a backward bifurcation under certain conditions.

LEMMA 5.3. *Assume that $B < 0$. If $N_y > 1$, $N_w < 1$, and $R_0 = 1$, then $\beta_x d_z > \beta_z d_x$.*

Proof. From (4.5) and (4.6), $R_0 = 1$ leads to

$$(5.5) \quad \lambda_x \beta_x d_z (1 - N_y) + \lambda_z \beta_z d_x (1 - N_w) < 0.$$

Furthermore, from (4.7), $R_0 = 1$ leads to

$$(5.6) \quad d_x d_z B = \beta_x^2 d_z^2 \lambda_x (N_y - 1) + \beta_z^2 d_x^2 \lambda_z (N_w - 1) < 0.$$

If $\beta_x d_z \leq \beta_z d_x$, multiplying the inequality (5.5) by $\beta_x d_z$, we deduce that

$$\lambda_x \beta_x^2 d_z^2 (1 - N_y) + \lambda_z \beta_z^2 d_x^2 (1 - N_w) < 0,$$

which contradicts (5.6). Thus, $\beta_x d_z > \beta_z d_x$ holds. \square

We state and prove the following theorem.

THEOREM 5.4. *If $R_0 = 1$ and $(N_y - 1)(N_w - 1) < 0$, then system (2.6) undergoes a backward bifurcation.*

Proof. We need to prove that a stable endemic equilibrium coexists with the stable DFE when $R_0 \leq 1$ and R_0 close to 1. Without loss of generality, we assume that $N_y > 1$ and $N_w < 1$.

We will prove that the endemic equilibrium E_M given by (5.4) is locally asymptotically stable for R_0 close to 1. The characteristic equation, associated to the equilibrium E_M , is given by $\Delta_{E_M}(\lambda) = 0$, where

$$(5.7) \quad \begin{aligned} \Delta_{E_M}(\lambda) = & (\lambda + d_x + \beta_x v_M)(\lambda + d_z + \beta_z v_M) \\ & \cdot (\lambda + \beta_x x_M + \beta_z z_M + u - \beta_x x_M N_y^\lambda - \beta_z z_M N_w^\lambda) \\ & + \beta_z^2 v_M z_M (\lambda + d_x + \beta_x v_M) (N_w^\lambda - 1) \\ & + \beta_x^2 v_M x_M (\lambda + d_z + \beta_z v_M) (N_y^\lambda - 1). \end{aligned}$$

First we prove that $\Delta_{E_M}(0) > 0$ for R_0 close to 1. We have $x_M = \frac{\lambda_x}{d_x + \beta_x v_M}$ and $z_M = \frac{\lambda_z}{d_z + \beta_z v_M}$; then

$$\begin{aligned} \Delta_{E_M}(0) &= \beta_x^2 v_M \lambda_x \frac{(d_z + \beta_z v_M)}{d_x + \beta_x v_M} (N_y - 1) + \beta_z^2 v_M \lambda_z \frac{(d_x + \beta_x v_M)}{d_z + \beta_z v_M} (N_w - 1) \\ &= \left(\beta_x \beta_z \lambda_x \left(\frac{\frac{d_z}{\beta_z} + v_M}{\frac{d_x}{\beta_x} + v_M} \right) (N_y - 1) + \beta_x \beta_z \lambda_z \left(\frac{\frac{d_x}{\beta_x} + v_M}{\frac{d_z}{\beta_z} + v_M} \right) (N_w - 1) \right) v_M \\ &= \left(\beta_x \beta_z \lambda_x (N_y - 1) \left(\frac{\frac{d_z}{\beta_z} + v_M}{\frac{d_x}{\beta_x} + v_M} \right)^2 + \beta_x \beta_z \lambda_z (N_w - 1) \right) \left(\frac{\frac{d_x}{\beta_x} + v_M}{\frac{d_z}{\beta_z} + v_M} \right) v_M. \end{aligned}$$

Thus, since $N_y > 1$ and $v_M > 0$, Lemma 5.3 implies that

$$\Delta_{E_M}(0) > (\beta_x \beta_z \lambda_x (N_y - 1) + \beta_x \beta_z \lambda_z (N_w - 1)) \left(\frac{\frac{d_x}{\beta_x} + v_M}{\frac{d_z}{\beta_z} + v_M} \right) v_M$$

for $R_0 = 1$. However, from (4.4), we deduce that

$$(5.8) \quad \lambda_x \beta_x \beta_z (N_y - 1) + \lambda_z \beta_x \beta_z (N_w - 1) > 0$$

whenever $B < 0$. Thus, for $R_0 = 1$ and $B < 0$, $\Delta_{E_M}(0) > 0$. By the continuity of $\Delta_{E_M}(\cdot)$ on all the parameters of system (2.6), we deduce that $\Delta_{E_M}(0) > 0$ for R_0 close to 1.

Now, consider $\Delta_{E_M}(\lambda)$ as a function of real λ . Notice that $\lim_{\lambda \rightarrow \infty} \Delta_{E_M}(\lambda) = +\infty$. The characteristic polynomial (5.7) can be written as

$$\begin{aligned} \Delta_{E_M}(\lambda) &= (\lambda + d_x + \beta_x v_M) (\lambda + d_z + \beta_z v_M) (\lambda + \beta_x x_M + \beta_z z_M + u) \\ &\quad - (\lambda + d_x) (\lambda + d_z + \beta_z v_M) N_y^\lambda \beta_x x_M - (\lambda + d_z + \beta_z v_M) \beta_x^2 x_M v_M \\ &\quad - (\lambda + d_z) (\lambda + d_x + \beta_x v_M) N_w^\lambda \beta_z z_M - (\lambda + d_x + \beta_x v_M) \beta_z^2 z_M v_M. \end{aligned}$$

Then one can see that $\lambda \mapsto \Delta_{E_M}(\lambda)$ is an increasing function. Thus, there exists a unique $\lambda^* < 0$ such that $\Delta_{E_M}(\lambda^*) = 0$. Separating real and imaginary parts in (5.7), one can show that all characteristic roots $\lambda \neq \lambda^*$ satisfy $\text{Re}(\lambda) < \lambda^*$. The calculation of this part is long and is omitted here. The local asymptotic stability of the endemic equilibrium E_M when R_0 nears 1 immediately follows from Theorem 2.1 in [5]. \square

6. Simulations. In this section, we provide some numerical simulations that support and extend our theoretical study for some particular values of the parameters.

We consider an explicit discretization of problem (2.1), based on backward Euler finite differences for the ODEs, a linearized finite difference method of characteristics for the PDE, and Simpson’s rule for the quadratures.

Let T be the final time of the simulation, and let h be the discretization step. Define $M_1 = \frac{\sup\{\theta: y_0(\theta) > 0\}}{h}$ and $M_2 = \frac{T}{h}$. It will be assumed, without loss of generality, that M_1 and M_2 are positive integers. We shall use the symbols $y_j^n, w_j^n, x^n, z^n, v^n$ to denote, respectively, the approximations of $y(jh, nh), w(jh, nh), x(nh), z(nh), v(nh)$.

Our numerical method, defined for $1 \leq n \leq M_2, 0 \leq j \leq M_1 + n$, is given by

$$(6.1) \quad \left\{ \begin{aligned} &\frac{y_j^n - y_{j-1}^{n-1}}{h} + [\eta_y(jh)y_j^n] = 0, \\ &y_0^n = \beta_x x^{n-1} v^{n-1}, \\ &\frac{x^n - x^{n-1}}{h} = \lambda_x - \beta_x x^n v^{n-1} - d_x x^n, \\ &\frac{w_j^n - w_{j-1}^{n-1}}{h} + [\eta_w(jh)w_j^n] = 0, \\ &w_0^n = \beta_x z^{n-1} v^{n-1}, \\ &\frac{z^n - z^{n-1}}{h} = \lambda_z - \beta_z z^n v^{n-1} - d_z z^n, \\ &\frac{v^n - v^{n-1}}{h} = \frac{h}{3} \sum_{j=0}^{M_1+n-2} (Y_j^n + W_j^n) - \beta_x x^{n-1} v^n - \beta_z z^{n-1} v^n - uv^n, \\ &Y_j^n = [k_y(jh)y_j^n + 4k_y(jh+h)y_{j+1}^n + k_y(jh+2h)y_{j+2}^n], \\ &W_j^n = [k_w(jh)w_j^n + 4k_w(jh+h)w_{j+1}^n + k_w(jh+2h)w_{j+2}^n]. \end{aligned} \right.$$

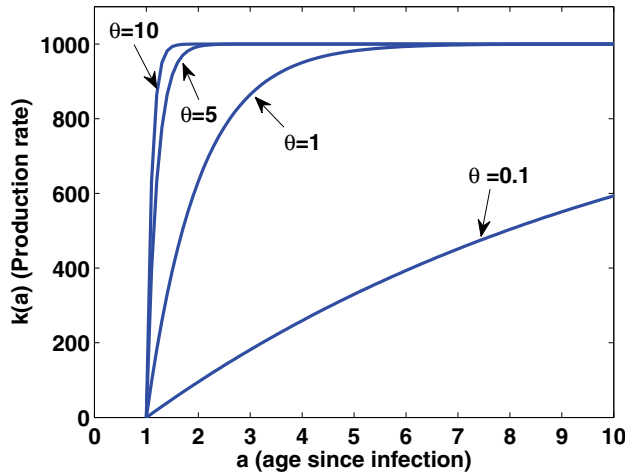


FIG. 3. Production rate of the virus for different values of θ .

We explore the behavior of the solution for a fairly realistic set of values of the relevant parameters, such as $d_x = 0.03 \text{ day}^{-1}$, $d_z = 0.03 \text{ day}^{-1}$, $\beta_x = 2 \times 10^{-10} \text{ ml}/(\text{virion-day})$, $\beta_z = 2 \times 10^{-10} \text{ ml}/(\text{virion-day})$, $\lambda_x = 10^8 \text{ cells}/(\mu\text{l-day})$, $\lambda_z = 10^5 \text{ cells}/(\mu\text{l-day})$. u is a free parameter which will be chosen to exhibit typical behaviors of the viral load concentration. For the production rate of the virus, we choose the following delayed exponential functions (see Nelson et al. [24] for more details):

$$(6.2) \quad k_y(a) = \begin{cases} k_{\max}^y (1 - e^{-\theta(a-a_1)}) & \text{if } a \geq a_1, \\ 0 & \text{else} \end{cases}$$

for the liver, and

$$(6.3) \quad k_w(a) = \begin{cases} k_{\max}^w (1 - e^{-\theta(a-a_1)}) & \text{if } a \geq a_1, \\ 0 & \text{else} \end{cases}$$

for the blood, where θ controls how rapidly the saturation levels, k_{\max}^y and k_{\max}^w , are reached, and a_1 represents a delay in viral production; that is, it takes time a_1 after initial infection for the first viral particles to be produced. This is displayed in Figure 3.

In our simulations, the parameter values are chosen as $k_{\max}^w = 0.01 \text{ virions}/\text{cell-day}$, $\theta = 0.1 \text{ day}^{-1}$, $a_1 = 0 \text{ days}$, whereas the maximal production rate k_{\max}^y is a free parameter that we will use to obtain different behaviors of the viral load.

In addition, the death rates, $\eta_y(a)$ and $\eta_w(a)$, of infected cells are supposed to be the same and, as in [24], are chosen as

$$(6.4) \quad \eta_y(a) = \eta_w(a) = \begin{cases} \eta_0 & \text{if } a < a_2, \\ \eta_0 + \eta_m (1 - e^{-\gamma(a-a_2)}) & \text{else,} \end{cases}$$

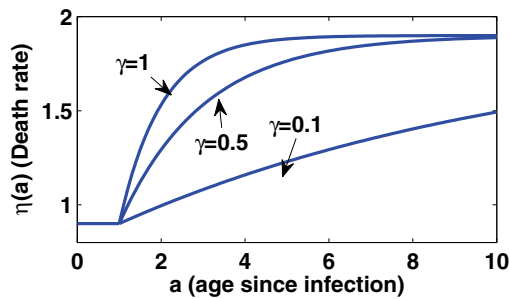


FIG. 4. Death rate of infected cells in the liver or in the blood for different values of γ .

where η_0 is the natural death rate of infected cells, $\eta_m + \eta_0$ is the maximal death rate, γ controls the time to saturation, and a_2 is the delay between infection and the onset of cell-mediated killing. This is displayed in Figure 4, where we choose $\eta_0 = 0.9 \text{ day}^{-1}$, $\eta_m = 1 \text{ day}^{-1}$, $a_2 = 0$ days.

We show in Figures 2–5 typical behaviors of the infected liver cells and viral load for different values of R_0 . In Figure 2, $R_0 = 0.97$, whereas $R_0 = 1.2$ in Figure 5A and $R_0 = 0.95$ in Figure 5B. One interesting feature of our model is that the disease does not necessarily die out when $R_0 \leq 1$. See Figure 2A in which we have $N_y < 1$, $N_w > 1$, and $R_0 = 0.97$. It is clear that in order to control the disease (i.e., the virus concentration declines to zero), we have to reduce the virus production in both the liver and the blood. In this case, the disease can be eradicated by reducing the value of the basic reproduction number R_0 below value 1 (see Figure 5B), and this can be achieved by reducing k_y and k_w or increasing η_y and η_w above certain critical values. Combination therapies, which reduce the rate of production in both the liver and the blood and at the same time increase the death and/or clearance rates of the infected cells or virus, could be much more effective than the current therapy, e.g., Interferon (IFN), which is assumed to be capable of blocking the production of new virions in the liver.

A question that arises from the backward bifurcation is “What is the lowest viral load needed to clear infection?” The parameters responsible for the appearance of the backward bifurcation allow the quantification of a threshold initial viral concentration, v_c , such that the virus in the blood and the liver is cleared if the viral concentration is below v_c and persists if it is above it. We illustrate this by simulating the infinite delay system (2.6) with the following set of parameter values: $d_x = 0.003 \text{ day}^{-1}$, $d_z = 0.03 \text{ day}^{-1}$, $\beta_x = 2 \times 10^{-10} \text{ ml}/(\text{virion-day})$, $\beta_z = 2 \times 10^{-10} \text{ ml}/(\text{virion-day})$, $\lambda_x = 10^8 \text{ cells}/(\mu\text{l-day})$, $\lambda_z = 10^5 \text{ cells}/(\mu\text{l-day})$, $u = 1 \text{ day}^{-1}$, $\eta_0 = 0.4 \text{ day}^{-1}$, $\eta_m = 1 \text{ day}^{-1}$, $\gamma_0 = 0$, $\theta_y = \theta_w = 1 \text{ day}^{-1}$, $a_1 = a_2 = 0$ days, $k_{max}^w = 1120 \text{ virions}/(\text{cell-day})$, and $k_{max}^w = 0.5264 \text{ virions}/(\text{cell-day})$. With this set of parameters, $N_y = 0.94$, $N_w = 2000$, and $R_0 = 0.9999992096$. A time series of the viral concentration v is shown in the top panel of Figure 6, showing the DFE (corresponding to $v = 0$) and two endemic equilibria (corresponding to $v_m = 6880158.520$ and $v_M = 22019841.48$). Further, Figure 6 shows that one of the endemic equilibria ($v_M = 22019841.48$) is locally asymptotically stable, the other ($v_m = 6880158.520$) is unstable (saddle), and the DFE is locally asymptotically stable. This clearly shows that disease elimination would depend on the initial size of the viral load in the liver and the blood. The associated bifurcation diagram is depicted in the bottom panel of Figure 6. Note that

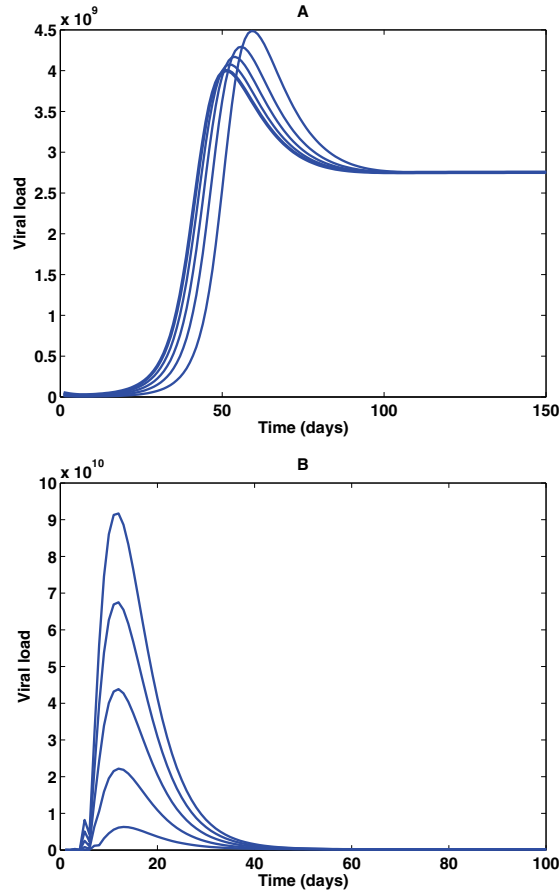


FIG. 5. Time series plot using different initial conditions for the initial viral load ($V_0 \in \{10^7, 2 \times 10^7, 3 \times 10^7, 4 \times 10^7, 5 \times 10^7\}$) (for curves from right to left) of system (2.1). Figure A corresponds to the stable endemic equilibrium for $R_0 = 1.2$, and Figure B corresponds to the stable DFE for $R_0 = 0.95$. The numbers that we chose reflect populations in one mL of blood.

since we simulated the infinite delay system (2.6), the initial conditions of viral load are functions of age since infection, $v(-a)$, $a \geq 0$, and give the viral load produced a day ago (produced by the infected cell, of age a , since its infection). In particular, this could be used to show the effect of age since infection on the elimination of the virus. In fact, since the viral load that is produced along the lifetime of an infected cell of age a is increasing by means of the age a , we assumed that the history function $v(-a)$, $a \geq 0$, is an exponential function given by $v(u) = \beta \exp(u)$, $u \leq 0$. As a consequence, simulations show that the viral load produced by infected cells declined to zero for $v(\cdot) \leq 462996 \exp(\cdot)$ and tended to the endemic equilibrium ($v_M = 22019841.48$) if $v(\cdot) > 462996 \exp(\cdot)$.

We also investigated the influence of the effect of the rate production on the behavior of viral load. More specifically, we studied changes in θ to determine how it affects the time to peak viral load (see Figure 7). We found that changes in θ led to a considerable variation in the time to the viral peak. When the production of new virus particles ramps up slowly ($\theta = 1/\text{day}$), the time to reach the peak viral load is

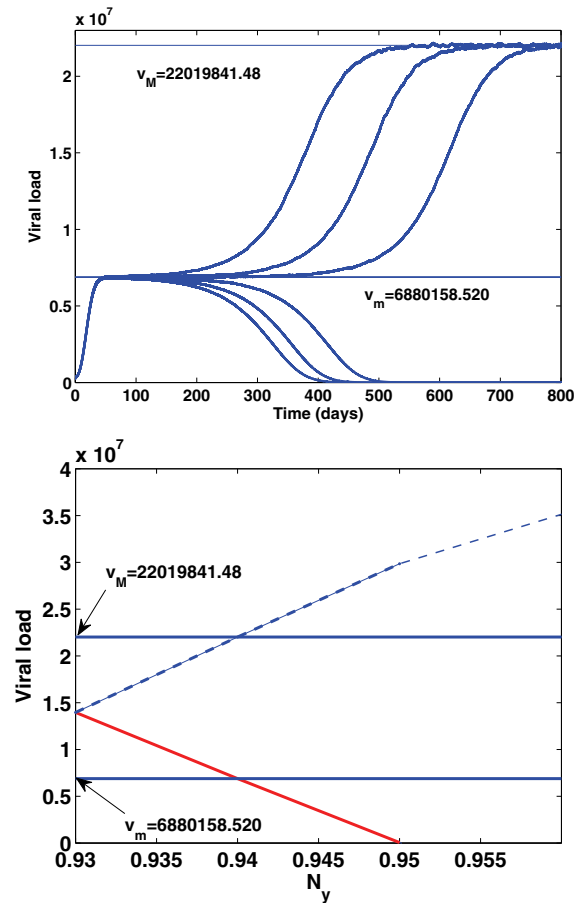


FIG. 6. Viral dynamics and bifurcation diagram. (Top) Time series plot, for model (2.6), using different initial conditions (functions) for the viral load (for $\theta \leq 0$, $V_0(\theta) \in \{462994 \exp(\theta), 462995 \exp(\theta), 462996 \exp(\theta), 462997 \exp(\theta), 462998 \exp(\theta), 462999 \exp(\theta)\}$). (Bottom) Bifurcation diagram showing a backward bifurcation and the endemic equilibria corresponding to $N_y = 0.94$ and the parameter values cited above. The numbers that we chose reflect populations in one mL of blood. Parameters used are given in the text.

delayed compared to when it ramps up faster ($\theta = 10/\text{day}$). However, for $\theta > 10/\text{day}$, the solution approximates the constant production case.

7. Discussions and conclusions. In this paper, we have developed a model of in-host HBV/HCV infection that incorporates a varying production rate of viral particles and an infected cell death rate which depends on age. The system leads to a system of differential equations with infinite delay. We have shown that several standard theorems in mathematical epidemiology can be extended to this kind of in-host model. The basic reproduction R_0 was also calculated, using the survival method described in [14].

Under certain conditions, the model has both a DFE which is stable when $R_0 < 1$ and unstable when $R_0 > 1$, and a stable endemic state when $R_0 > 1$, similar to the basic one compartment model. The epidemiological implication of this result is that, in general, when R_0 is less than unity, a small influx of virus particles into the liver

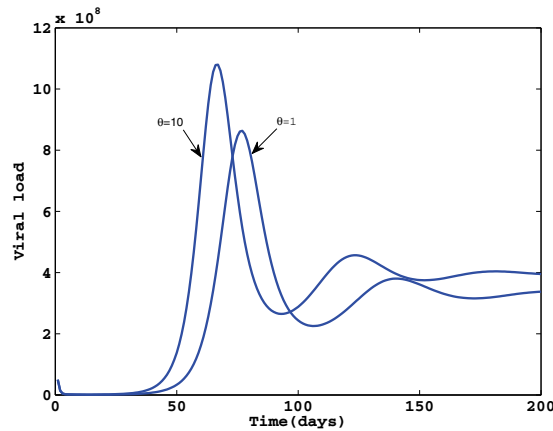


FIG. 7. Change in viral load peak depending on θ . Numerical simulations show that the peak viral load magnitude, and the time of this peak, change with different values of the parameter θ . The numbers that we chose reflect populations in one mL of blood.

and the blood would not generate infection, and the disease dies out in time (since the DFE is globally asymptotically stable). Furthermore, the disease persists when R_0 is larger than unity. However, under other conditions, a backward bifurcation exists in our model, which means that reducing the basic reproduction number R_0 below 1 is not always sufficient to eliminate the HBV/HCV infection when the virus interacts in both the liver and the blood.

One can observe that when the production rates of the virus and the death rates of infected cells in the liver and the blood are constants, the model (2.1) reduces to the system of ODEs modeled and analyzed by Qesmi et al. [30]. The model (2.1), however, gives a more realistic description of the infection process by including a varying virus production rate and an infected cell death rate depending on the age of infection of an infected cell. Both the current model and the ODE model of Qesmi et al. [30] demonstrate backward bifurcations, leading to important conclusions regarding drug efficacy in both the blood and the liver.

In the current model, backward bifurcation is only possible if $(N_y - 1)(N_w - 1) < 0$. Briefly, this means that if drug therapy is effective in reducing $N_y < 1$ in the liver, but is not successful in reducing $N_w < 1$ in the blood (and vice versa), the virus can not be eradicated even if the basic reproduction number R_0 is reduced below 1. From Theorem 4.2, we have explicit expressions to guarantee that no backward bifurcation occurs. In fact, for $(N_y - 1)(N_w - 1) \geq 0$, the viral particles as well as the infected cells die out once the value of R_0 is below 1. Moreover, the bifurcation is always forward for $N_y \geq 1$ and $N_w \geq 1$. A more possible interpretation of this phenomenon in our model would be that the virus persists (the equilibrium moves away from the DFE) when either the liver or the blood compartment absorbs more virus than it produces and that the absorbed virus quantity exceeds a critical threshold of the virus (see Figure 5A). This type of dynamic is likely related to the innate immune-response phenomenon which is the first line of defense against infectious diseases [32]. This particular issue is important and not addressed here but will be studied in depth in future work.

In future work the current model will be employed to study the reinfection dy-

namics of a new liver in a transplant patient. This will include the effects of drug therapy and immunosuppressive drugs (so that the new liver will not be rejected). Such a study will enable us to determine the proportion of HBV/HCV infection that occurs in the blood and thus will have important implications for the development of new drug therapies or vaccines which need to be effective in both the liver and blood compartments.

The current viral dynamic model ignores some immunological and pharmacokinetic effects that could play a major role in the assessment of the true decay rate of free virus in each of the liver and the blood compartments. For example, the dynamics of the CD8 T-cell population, which is responsible for killing infected cells, is ignored. Also, the pharmacokinetic effects of taking drug therapy in doses is not included in our model. Thus, an important extension of the current work would include these effects into our model. Note that, in these cases, it may be necessary to split the virus compartment into two subcompartments that capture CD8 T-cell dynamics and drug absorption in the liver and the blood separately.

Finally, one can note that our model can be easily extended to incorporate lytic viruses, where the lifetime of infected cells is affected by the infection process. Note that lytic viruses may also change the production dynamics of new virus particles, where these particles are released in one big burst, when the infected cell dies or is killed. This is a project for future work.

Acknowledgment. The authors thank the anonymous referees, whose careful reading, insights, valuable comments, and suggestions significantly enabled us to improve the quality of the paper.

REFERENCES

- [1] P. CACOUB AND B. TERRIER, *Hepatitis B-related autoimmune manifestations*, *Rheumatic Disease Clinics of North America*, 35 (2009), pp. 125–137.
- [2] A. D. COOMBS, M. GILCHRIST, J. PERCUS, AND A. PERELSON, *Optimal viral production*, *Bull. Math. Biol.*, 65 (2003), pp. 1003–1023.
- [3] G. COQUILLARD AND B. K. PATTERSON, *Determination of hepatitis C virus-infected, monocyte lineage reservoirs in individuals with or without HIV coinfection*, *J. Infect. Dis.*, 200 (2009), pp. 947–954.
- [4] S. E. DAVIES, B. C. PORTMANN, O'J. G. GRADY, P. M. ALDIS, K. CHAGGAR, G. J. ALEXANDER, AND R. WILLIAMS, *Hepatic histological findings after transplantation for chronic hepatitis B virus infection, including an unique pattern of fibrosing cholestatic hepatitis*, *Hepatology*, 13 (1991), pp. 150–157.
- [5] W. DESCH AND W. SCHAPPACHER, *Linearized stability for nonlinear semigroups*, in *Differential Equations in Banach Spaces, Lecture Notes in Math.* 1223, A. Favini and E. Obrecht, eds., Springer, New York, 1986, pp. 61–73.
- [6] O. DIEKMANN, J. A. P. HEESTERBEEK, AND J. A. J. METZ, *On the definition and computation of the basic reproduction ratio R_0 in models for infectious diseases in heterogeneous populations*, *J. Math. Biol.*, 28 (1990), pp. 365–382.
- [7] P. VAN DEN DRIESSCHE AND J. WATMOUGH, *Reproduction number and sub-threshold endemic equilibria for compartmental models of disease transmission*, *Math. Biosci.*, 180 (2002), pp. 29–48.
- [8] Z. FENG, C. CASTILLO-CHAVEZ, AND A. CAPURRO, *A model for tuberculosis with exogenous reinfection*, *Theoretical Population Biology*, 57 (2000), pp. 235–247.
- [9] B. N. FIELDS, D. M. KNIPE, P. M. HOWLEY, R. M. CHANOCK, T. P. MONATH, J. L. MELNICK, B. ROIZMAN, AND S. E. STRAUS, *Fields Virology*, 3rd ed., Lippincott Williams & Wilkins, Philadelphia, 1996.
- [10] M. W. FRIED, M. L. SHIFFMAN, K. R. REDDY, C. SMITH, G. MARINOS, JR., F. L. GONCALES, D. HÄUSSINGER, M. DIAGO, G. CAROSI, D. DHUMEAUX, A. CRAXI, A. LIN, J. HOFFMAN, AND J. YU, *Peginterferon alfa-2a plus ribavirin for chronic hepatitis C virus infection*, *N. Engl. J. Med.*, 347 (2002), pp. 975–982.

- [11] L. GRELLIER, D. MULTIMER, M. AHMED, D. BROWN, A. K. BURROUGHS, K. ROLLES, P. MCMASTER, P. BERANEK, F. KENNEDY, H. KIBBLER, P. MCPHILLIPS, E. ELIAS, AND G. DUSHEIKO, *Lamivudine prophylaxis against reinfection in liver transplantation for hepatitis B cirrhosis*, *Lancet*, 1 (1996), p. 1212.
- [12] H. GOMEZ-ACEVEDO AND M. Y. LI, *Backward bifurcation in a model for HTLV-I infection of CD4+ T cells*, *Bull. Math. Biol.*, 67 (2005), pp. 101–114.
- [13] K. HADELER AND P. VAN DEN DRIESSCHE, *Backward bifurcation in epidemic control*, *Math. Biosci.*, 146 (1997), pp. 15–35.
- [14] J. M. HEFFERNAN, R. J. SMITH, AND L. M. WAHL, *Perspectives on the basic reproductive ratio*, *J. R. Soc. Interface*, 2 (2005), pp. 281–293.
- [15] J. M. HEFFERNAN AND L. M. WAHL, *Monte Carlo estimates of natural variation in HIV infection*, *J. Theoret. Biol.*, 236 (2005), pp. 137–153.
- [16] J. M. HEFFERNAN AND L. M. WAHL, *Improving estimates of the basic reproductive ratio: Using both the mean and the dispersal of transition times*, *Theoretical Population Biology*, 70 (2006), pp. 135–145.
- [17] F. HOLLINGER AND T. LIANG, *Hepatitis B virus*, in *Fields Virology*, 4th ed., D. M. Knipe et al., eds., Lippincott Williams & Wilkins, Philadelphia, 2001, pp. 2971–3036.
- [18] K. K. HOLMES, P. F. SPARLING, W. E. STAMM, P. PIOT, J. N. WASSERHEIT, L. COREY, M. S. COHEN, AND D. H. WATTS, *Sexually Transmitted Diseases*, 4th ed., McGraw-Hill, Toronto, Canada, 2008.
- [19] M. IANNELLI, *Mathematical Theory of Age-Structured Population Dynamics*, Applied Mathematics Monographs 7, Comitato Nazionale per le Scienze Matematiche, Consiglio Nazionale delle Ricerche (C.N.R.), Giardini, Pisa, 1995.
- [20] C. M. KRIBS-ZALETA AND M. MARTCHEVA, *Vaccination strategies and backward bifurcation in an age-since-infection structured model*, *Math. Biosci.*, 177–178 (2002), pp. 317–332.
- [21] T. LASKUS, M. RADKOWSKI, J. WILKINSON, H. VARGAS, AND J. RAKELA, *The origin of hepatitis C virus reinfecting transplanted livers: Serum-derived versus peripheral blood mononuclear cell-derived virus*, *J. Infect. Dis.*, 185 (2002), pp. 417–421.
- [22] M. P. MANNS, J. G. MCHUTCHISON, S. C. GORDON, V. K. RUSTGI, M. SHIFFMAN, R. REINDOLLAR, Z. D. GOODMAN, K. KOURY, M. LING, AND J. K. ALBRECHT, *Peginterferon alfa-2b plus ribavirin compared with interferon alfa-2b plus ribavirin for initial treatment of chronic hepatitis C: A randomised trial*, *Lancet*, 358 (2001), pp. 958–965.
- [23] R. K. MILLER, *Nonlinear Volterra Integral Equations*, W. A. Benjamin, New York, 1971.
- [24] P. W. NELSON, M. A. GILCHRIST, D. COOMBS, J. M. HYMAN, AND A. S. PERELSON, *An age-structured model of HIV infection that allows for variations in the production rate of viral particles and the death rate of productively infected cells*, *Math. Biosci. Eng.*, 1 (2004), pp. 267–288.
- [25] M. A. NOWAK, S. BONHOEFFER, A. M. HILL, R. BOEHME, H. C. THOMAS, AND H. MCDADE, *Viral dynamics in hepatitis B virus infection*, *Proc. Natl. Acad. Sci. USA*, 93 (1996), pp. 4398–4402.
- [26] M. A. NOWAK AND R. M. MAY, *Virus Dynamics*, Oxford University Press, Oxford, UK, 2000.
- [27] A. S. PERELSON AND P. W. NELSON, *Mathematical analysis of HIV-1 dynamics in vivo*, *SIAM Rev.*, 41 (1999), pp. 3–44.
- [28] A. PERELSON, A. NEUMANN, M. MARKOWITZ, J. LEONARD, AND D. HO, *HIV-1 dynamics in vivo: Virion clearance rate, infected cell life-span, and viral generation time*, *Science*, 271 (1996), pp. 158–286.
- [29] PUBLIC HEALTH AGENCY OF CANADA, *Hepatitis B fact sheet*, <http://www.phac-aspc.gc.ca/tmp-pmv/info/hep-b-eng.php> (2009).
- [30] R. QESMI, J. WU, J. WU, AND J. M. HEFFERNAN, *Influence of backward bifurcation in a model of hepatitis B and C viruses*, *Math. Biosci.*, 224 (2010), pp. 118–125.
- [31] T. C. RELUGA, J. MEDLOCK, AND A. S. PERELSON, *Backward bifurcations and multiple equilibria in epidemic models with structured immunity*, *J. Theoret. Biol.*, 252 (2008), pp. 155–165.
- [32] A. REYNOLD, J. RUBINA, G. CLERMONTB, J. DAYA, Y. VODOVOTZB, AND G. B. ERMENTROUT, *A reduced mathematical model of the acute inflammatory response: I. Derivation of model and analysis of anti-inflammation*, *J. Theoret. Biol.*, 242 (2006), pp. 220–236.
- [33] M. RONT, T. ASSELAH, V. PARADIS, N. MICHOUX, M. DORVILLIUS, G. BARON, P. MARCELLIN, B. E. VAN BEERS, AND V. VILGRAIN, *Virus infection: Differentiating minimal from intermediate fibrosis with perfusion CT*, *Radiology*, 256 (2010), pp. 135–142.
- [34] H. R. THIEME, *Persistence under relaxed point-dissipativity (with application to an endemic model)*, *SIAM J. Math. Anal.*, 24 (1993), pp. 407–435.

- [35] M. TSIANG, J. ROONEY, J. TOOLE, AND C. GIBBS, *Biphasic clearance kinetics of hepatitis B virus from patients during adefovir dipivoxil therapy*, *Hepatology*, 29 (1999), pp. 1863–1869.
- [36] G. WEBB, *Theory of Nonlinear Age-Dependent Population Dynamics*, Marcel Dekker, New York, 1985.
- [37] C. WEIDEKAMM ET AL., *Effects of TIPS on liver perfusion measured by dynamic CT*, *American Journal of Roentgenology*, 184 (2005), pp. 505–510.
- [38] WORLD HEALTH ORGANIZATION, *Heptatitis B fact sheet*, no. 204, <http://www.who.int/mediacentre/factsheet/fs204/en/>, 2000.